Int. J. Electrochem. Sci., 16 **(2021)** 150956, doi: 10.20964/2021.01.09

International Journal of
ELECTROCHEMICAL
SCIENCE
www.electrochemsci.org

A Reusable Electrochemical Aptasensor for the Sensitive Detection of Pb(II) with an Electrodeposited AuNP-Modified Electrode based on the Formation of a Target-Induced G-Quadruplex

Guo Zhao[1], *Cong Li*[2], *Xiaochan Wang*[3], *Gang Liu*[4,5,*], *Nguyen Thi Dieu Thuy*[3]

[1] College of Artificial Intelligence, Nanjing Agricultural University, Nanjing, 210031, PR China
[2] NARI Technology Development Co. Ltd., Nanjing, 210061, PR China
[3] College of Engineering, Nanjing Agricultural University, Nanjing, 210031, PR China
[4] Key Lab of Modern Precision Agriculture System Integration Research, Ministry of Education of China, China Agricultural University, Beijing 100083 P.R. China
[5] Key Lab of Agricultural Information Acquisition Technology, Ministry of Agricultural of China, China Agricultural University, Beijing 100083 P.R. China
[*]E-mail: pac@cau.edu.cn

Received: 3 September 2020 / *Accepted:* 21 October 2020 / *Published:* 30 November 2020

A label-free and reusable electrochemical aptasensor for Pb(II) detection using the G-quadruplex-Pb(II) binding interaction and target-induced strand release is proposed. This strategy is based on the changes in the electrochemical impedance spectroscopy (EIS) results caused by the separable structure of aptamer DNA rich in guanine. Additionally, a controllable gold nanoparticle (AuNP) layer was electrochemically reduced on a glassy carbon electrode (GCE) surface as the modified substrate for aptamer DNA. The AuNPs provided a large surface area and more active sites during immobilization and hybridization, which enhanced the EIS signal. In the presence of Pb(II), the EIS intensity of the aptasensor decreased significantly due to the special interaction between Pb(II) and G4-DNA, which prompted the aptamer to construct a G-quadruplex and caused the two DNA strands to untwist. This untwisting resulted in the release of G4-DNA. The aptamer probe structure of the double strand was then altered to a single strand because of the formation of the Pb(II)-G-quadruplex compound by the binding of Pb(II) on the aptamer. This binding changed the electron transfer kinetics between the surface of the electrode and the aptamer DNA strand, leading to a decrease in the EIS response. Results show that the charge transfer resistance decreased linearly and proportionally to the log function of the Pb(II) concentration from 0.001 to 100 μg/L. Moreover, the developed aptasensor demonstrated a high selectivity toward Pb(II), and the calculated detection limit was 0.0046 nM (S/N = 3), which indicated that our proposed electrochemical aptasensor was capable of Pb(II) detection at a trace level.

Keywords: Electrochemical impedance spectroscopy, biosensor, target-induced strand release, Pb(II) detection, gold nanoparticles, electrochemical aptasensor

1. INTRODUCTION

Currently, heavy metal contamination is the cause of many serious and fatal diseases worldwide because of its high toxicity and nonbiodegradability. Particularly, Pb(II) causes various neurotoxic effects due to its combination with various amino acids, thereby resulting in the prevention of normal physiological activities. Additionally, the presence of Pb(II) in the environment can accumulate in the human body due to amplification up the food chain. This accumulation can damage physiological systems, including the kidneys, reproductive system and nervous system, which potentially cause anemia and high blood pressure. Therefore, the ability to analyze the Pb(II) concentration is in huge demand to monitor drinking water and food safety, and this analysis may be a useful tool for the control and prevention of Pb(II) pollution. Compared to some conventional detection techniques, for instance, atomic absorption spectroscopy (AAS) [1], inductively coupled plasma-atomic emission spectrometry (ICP-AES) [2], electrochemical techniques [3-5] and inductively coupled plasma-mass spectrometry (ICP-MS) [6-9], electrochemical techniques, e.g., cyclic voltammetry (CV) and electrochemical impedance spectroscopy (EIS), afford the outstanding advantages of a quick response, simplicity of use, low cost and high sensitivity; thus, these techniques are widely used in electrochemical sensors and biosensors [10-12], including enzyme sensors, immunosensors and aptasensors.

As one kind of artificial nucleic acid sequence, aptamers have been widely investigated and used in the areas of nanotechnology, biological engineering and bioassays [13,14] owing to their excellent characteristics, such as their easy modifiability, simple in vitro screening, and high diversity, along with their good chemical stability and affinity as inherent properties. To date, biosensors modified with aptamers, i.e., aptasensors, have been successfully fabricated and further applied for the determination of various targets, such as whole cells [15], large biological molecules [16] and small molecules [17]. Due to the inherent advantages of aptasensors based on electrochemical techniques, including their high stability, low cost, high sensitivity and simplicity, aptasensors have been increasingly studied in the biosensing field.

The detection process of aptasensors can be significantly simplified based on the application of electrochemical techniques [18]. In addition, the electrochemical technique enables the miniaturization of the analytical device and consequently decreases the consumption of aptamers [19]. In particular, the electrochemical response caused by the combination of target molecules with aptamers provides the basic detection principle for analytical devices [20]. Owing to the excellent performance of the electrochemical technique-based aptasensors discussed above, they can be used for the sensitive, simple, selective, rapid and label-free determination of target analytes [21,22]. EIS, as one of the electrochemical techniques, has been used as an effective means to monitor the peculiarities of electron transfer kinetics on the surface of modified electrodes [23]. EIS-based biosensors afford many advantages, such as their ability to be used with label-free aptamers [24], electrochemical response quantification, minimal interference with the biological binding process and ability to identify surface binding events that relying on the charge transfer resistance.

In regard to the fabrication of electrochemical technique-based aptasensors, a variety of solid substrates have been used. Among the different substrates, gold was one of the most popular solid surfaces, which can be attributed to the physisorption between gold and an aptamer [25], avidin–biotin

binding [26], attraction to the monolayer of a cysteamine intermediate [27], and covalent bonding and conjugation via thiol and phosphorothioate groups [28,29]. Au nanoparticle (AuNP)-modified electrodes have been successfully applied in the fabrication of biosensors and electrochemical sensors because of their remarkable chemical and physical properties [30–32]. Moreover, AuNPs have been broadly applied in the fabrication of electrochemical technique-based aptasensors [33–35]. Based on the AuNP layer modified on the surface of the electrode, linkers used for the capture of the aptamer can be modified on the surface of the electrode due to the strong affinity of the SH–Au covalent linkages [36–38]. Considering the drawbacks of gold electrodes used for the fabrication of aptasensors with a small specific surface area, in this paper, glassy carbon electrodes (GCEs) modified with AuNPs were used to develop label-free and reusable electrochemical aptasensors instead of gold electrodes, which provided an enhanced electrochemical response of hybridization and a high specific surface area.

In the last few decades, many biosensors with a high selectivity and sensitivity for Pb(II) detection have been proposed by the cleaving reaction with a Pb(II)-specific RNA-cleaving DNAzyme being converted into electrochemical [39], luminescent, colorimetric [40] or fluorescent signals [41]. Regardless, its further application was limited not only by the low stability of Pb(II)-specific DNAzymes but also by the high cost of DNAzyme synthesis. As an alternative, aptamers with an allosteric G-quadruplex formed by the induction of Pb(II) can be expected to be designed as a new sensing element with high specificity, in which the changes of the conformation are measured by electrochemical techniques, the naked eye or spectrometry [42,43].

In this study, a selective and sensitive electrochemical aptasensor based on the strategy of a Pb(II)-induced strand release using a G-rich Pb(II)-induced allosteric aptamer was proposed for the determination of Pb(II). Additionally, glassy carbon was used as the substrate for the modification of the AuNP layer by electrochemical deposition, which provided a large specific surface area and abundant active sites for the immobilization of single-strand DNA as a capture probe. Consequently, the single-strand Pb(II)-specific aptamer was hybridized with the single-strand capture probe to form a double helix structure. Upon the addition of Pb(II), the double helix structure was induced to unwind, and a G-quadruplex aptamer was formed. Subsequently, the produced G-quadruplex-Pb(II) was released from the electrode surface based on the cleavage of the double helix structure, which was caused by the induction of Pb(II) and altered the charge transfer resistance (Rct). Thus, the concentration of Pb(II) was expected to be detected selectively and sensitively based on the relative change in Rct with a limit of detection of 0.0046 nM. The electrochemical aptasensor for Pb(II) detection proposed in this study can be expected to be used as a reference mode for a variety of target analytes.

2. EXPERIMENTAL

2.1 Reagents and instruments

The following DNA sequences were obtained from Shanghai Sangon Biological Engineering Technology & Service Co., Ltd (China), G4-DNA: 5'-TGGGTGGGTGGGTGGG-3', CS-DNA: 5'-NH_2-CCCACCCACCCTTTTT-3', CS0-DNA: 5'-NH_2-CCCACCCACCCACCCA-3', CS1-DNA: 5'-NH_2-CCCACCCACCCATTTT-3', CS2-DNA: 5'-NH_2-CCCACCCACCCTTTTT-3', CS3-DNA: 5'-

NH_2-CCCACCCACCTTTTTT-3', CS4-DNA: 5'-NH_2-CCCACCCACTTTTTTT-3', CS5-DNA: 5'-NH_2-CCCACCCATTTTTTTT-3', NS-DNA: 5'- AAAAATGGGTGTGA-3'.

$HAuCl_4 \cdot 3H_2O$ and ethanolamine (EA), methylphosphonic acid (MPA) and bovine serum albumin (BSA) were used without further purification and were purchased from Sigma-Aldrich (USA). Ethanolamine (EA), N-hydroxysulfosuccinimide (NHS) and (1-ethyl-3-(3-dimethylaminopropyl) carbodiimide hydrochloride) (EDC) were purchased from Fisher Scientific (USA). A platinum wire counter electrode (CE), a Ag/AgCl reference electrode (RE) and a AuNP-modified GCE (Φ = 3 mm) were used to construct a three-electrode system for the electrochemical analysis of the proposed aptasensor. A phosphate buffer (10 mM, pH 7.4) was used to prepare the DNA solution at a concentration of 100 μM as the stock solution. Then, the obtained solution was heated to 80 °C for 5 min to avoid aggregation and dissociate the intermolecular interaction between DNA strands, respectively. Consequently, a solution of uniform single-stranded DNA was obtained by gradually cooling the solution down to 25 °C [44]. An electrochemical workstation (CH Instrument 660E, Shanghai CH Instruments) was used to perform the electrochemical impedance analysis.

2.2 Modification of the electrode

Prior to the electrode modification, the surface of the GCE was polished with alumina powder (0.3 μm). After that, the surface of the obtained electrode was cleaned by sonication in 0.01 M nitric acid, absolute ethyl alcohol and Milli-Q water. A controllable and feasible method that was based on electrochemical deposition was used for modifying the bare GCE surface with a the AuNP layer. The electrochemical deposition was performed in a 0.1 mM $HAuCl_4$ solution using cyclic voltammetry at a sweep rate of 0.05 V/s from -1.2 to -0.8 V with a sweep segment of 20 a 0.1 M phosphate-buffered saline solution at pH 9.0. A AuNPs/GCE was obtained after drying in a nitrogen atmosphere.

2.3 Fabrication of the aptasensor

The fabrication procedure of the proposed aptasensor was described as follows: First, MPA was immobilized on the surface of AuNPs/GCE based on the covalent binding of SH–Au. EDC/NHS chemistry was used to covalently modify CS-DNA on the electrode surface based on the carboxylic groups from MPA/AuNPs/GCE. MPA/AuNPs/GCE was immersed in a 20 mg/mL EDS solution that was prepared by dissolving in a 0.1 M MES solution at pH 6.0 for 30 min. Then, EDC/MPA/AuNPs/GCE was transferred to a 0.1 M MES solution at pH 6.0 that contained 20 mg/mL NHS for 20 min to activate the carboxylic groups; thus, NHS/EDC/MPA/AuNPs/GCE was obtained. The quenching of the unreacted–NHS was completed by pipetting 10 μL of 0.1 M EA on the surface of NHS/EDC/MPA/AuNPs/GCE to obtain EA/NHS/EDC/MPA/AuNPs/GCE. In addition, blocking of the free AuNP surface was achieved by pipetting 10 μL of 30 μM BSA on the surface of EA/NHS/EDC/MPA/AuNPs/GCE. The solutions of EA and BSA were prepared by using a 10 mM PB solution at a pH of 7.4, and the washing process was carried out using 10 mM PB after quenching and blocking. After that, G4-DNA was hybridized with the CS-DNA immobilized on the electrode surface by incubating the obtained electrode with 10 μL of a 100 nM G4-DNA solution for 150 min to construct

a DNA duplex at room temperature. Additionally, the used aptasensor was reactivated by incubating the electrode with 10 μL of a 100 nM G4-DNA solution for 40 min after each measurement to again immobilize G4-DNA (Fig. 1).

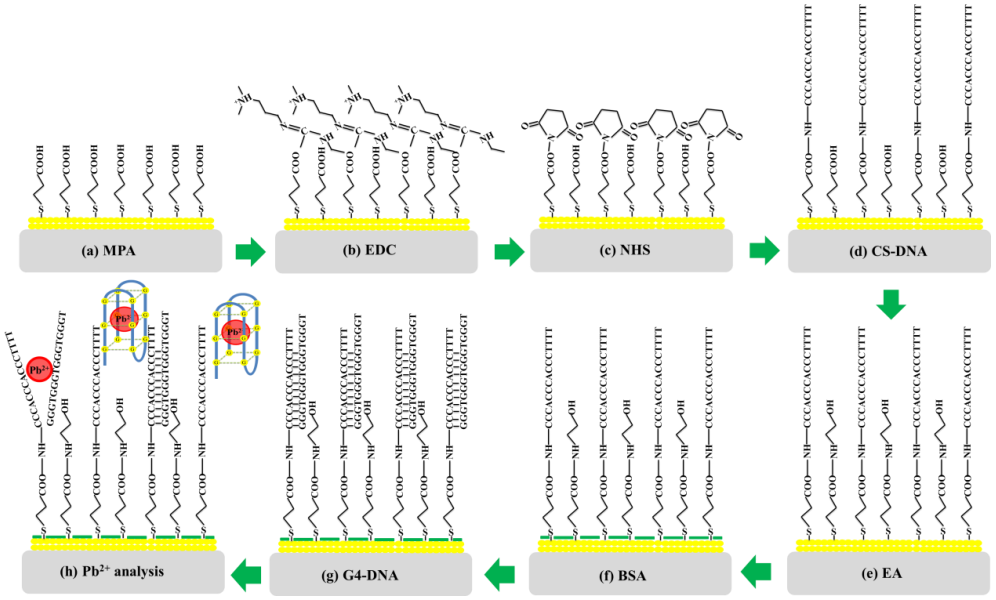

Figure 1. Schematic showing the device fabrication and sensing protocol.

2.4 EIS Measurements

All electrochemical EIS analyses were performed at room temperature by an electrochemical workstation based on a three-electrode system consisting of a platinum wire CE, a Ag/AgCl RE and the aptamer-modified AuNPs/GCE as the working electrode (WE). $K_3[Fe(CN)_6]$ (0.1 mM) prepared in 10 mM PBS at pH 7.4 was used as a redox probe. A DC potential of 0.19 V and a frequency range of 0.1 Hz to 100 kHz were selected to measure the EIS response of the proposed aptasensor. The Rct values were obtained by the equivalent circuit, which was obtained by simulating the electrochemical impedance spectroscopy results with a modified Randles circuit.

2.5 Principle of sensing

To detect the Pb(II) concentration, the aptasensor as the working electrode was immersed in a 10 mM PBS solution at pH 7.4 containing 0.1 mM $K_3[Fe(CN)_6]$, and the initial Rct was measured. The Rct was calculated using the representative Nyquist plots with the equivalent circuit. Subsequently, the proposed aptasensor was incubated in 1 mL of Pb(II) solution at room temperature for 40 min and then washed with PB solution three times to wash away the Pb(II) residue. Next, the washed electrode was again immersed in the above PB buffer, and the Rct was measured. The modified electrode was reused by moving the electrode to the G4-DNA solution for 40 min after detection. To obtain reliable results, each measurement was carried out with three electrodes, and the relative change in Rct was calculated using the following equation:

Relative Rct = (Rct0−Rct)/Rct0 × 100 %

where Rct0 is the initial charge transfer resistance of the surface of the modified electrode and R is the Rct after the modified electrode surface is exposed to the Pb(II) solution. The value of Rct between the $[Fe(CN)_6]^{3-/4-}$ redox probe and the modified electrode surface could be affected by the formation of the Pb(II)-G-quadruplex complex based on a special interaction between G4-DNA and Pb(II). Therefore, the concentration of Pb(II) could be detected by monitoring the relative change in Rct based on the mathematical relationship between the redox probe and modified electrode surface.

3. RESULTS AND DISCUSSION

3.1 Modeling of the Nyquist Curves

The EIS responses over a frequency range of 0.1 Hz to 100 kHz for different concentrations of Pb(II) are shown in Fig. 2. The modeling of the Nyquist curves was performed by the EIS simulation based on a modified Randles circuit. As shown in Fig. 2, there are two semicircles with different diameters distributed in the low- and high-frequency regions. The small semicircle observed in the high-frequency region represents the impedance caused by events in the AuNP layer, whereas the semicircle with a large diameter, observed in the low-frequency region, represents the impedance resulting from surface processes.

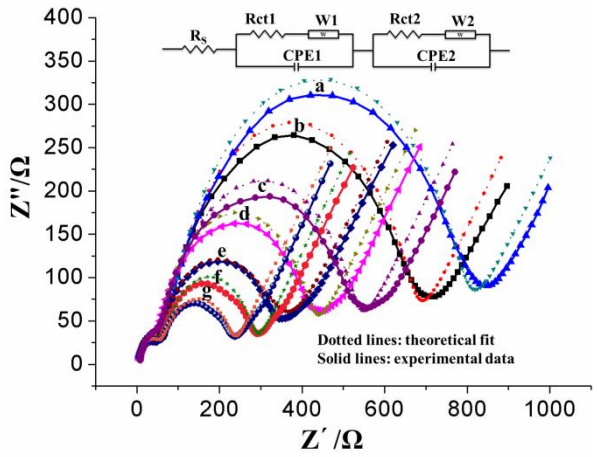

Figure 2. Nyquist curves at different Pb(II) concentrations: (**a**) 0, (**b**) 1, (**c**) 10, (**d**) 10^2, (**e**) 10^3, (**f**) 10^4 and (**g**) 10^5 ng/L. The dotted lines are the experimental data, and the solid lines are the theoretical curves based on the modified Randles circuit. The inset is the modified Randles circuit representing the equivalent circuit model to fit the Nyquist curves of the EIS measurements.

A similar phenomenon can be observed on the paper published by Gang Liang et al [45]. They proposed a sensing assay for ethanolamine detection by combining G-rich aptamer DNA with EIS, in which Rct was increased with the increase of ethanolamine concentration by using the $[Fe(CN)_6]^{3-/4-}$ as a redox probe. The EIS obtained in this study shows that the diameter of the small semicircle remained almost constant, while the diameter of the large semicircle decreased as the Pb(II) concentration increased. This result could be explained by the equivalent circuit model shown in the inset of Fig. 2. CPE2 and Rct2 shown in Fig. 2 are the double layer capacitance and charge transfer resistance on the

surface of the modified electrode, respectively, which to some extent was consistent with the equivalent circuit model used by Rui-Guo Cao et al. for low frequency area [46]. However, there was a difference in the area of high frequency as compared with literature described above, which CPE1 and Rct1 shown in Fig. 2 represent the charge diffusion in the space charge layer and the electron transfer kinetics in the AuNP layer, respectively. In addition, W1 and W2 are the Warburg impedance values. The similar results and principle can be found in the paper reported by Saeromi Chung et al. [47].

3.2 Characterization of the modified electrode

The SEM image of the electrochemically deposited AuNPs on the GCE is shown in Fig. 3, which shows that a large number of AuNPs were uniformly distributed on the surface of the GCE, and these AuNPs had an average diameter of ~60 nm. The deposition of AuNPs increased the specific surface area of the GCE and supplied more attachment sites for the modification of the aptamer, thereby enabling the good sensitivity of the proposed aptasensor [48,49]. Qing Xu et al. also further confirmed the application prospect of AuNPs in the fabrication of molecular beacon-based biosensors [50].

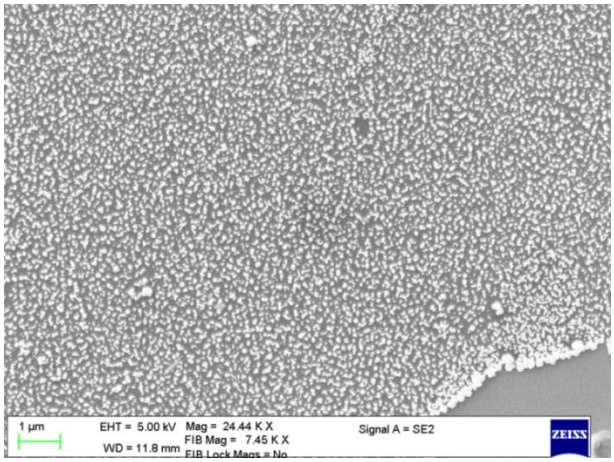

Figure 3. SEM image of the AuNP-modified GCE

The specific interaction during each modification was further confirmed by the investigation of Rct based on the representative Nyquist plots, as shown in Fig. 4. The Nyquist plot of the modified electrode was used to measure the Rct at each modification step in the redox probe solution composed of 10 mM PBS and 0.1 mM $[Fe(CN)_6]^{3-/4-}$ at a pH of 7.4. The Rct of the electrode surface was only 40.81 Ω after the deposition of AuNPs on the GCE due to the good electron transfer ability of gold. The Rct increased gradually to 60.34, 64.92, and 74.53 Ω after the immobilization of MPA/EDC/NHS, CS-DNA and EA, respectively. Moreover, the Rct increased significantly from 74.53 to 114.55 and then to 674.5 Ω after the sequential immobilization of BSA and G4-DNA, resulting from the interference of biomolecules with a charge transfer, which blocked the redox process of the $[Fe(CN)_6]^{3-/4-}$ probes on the

surface of the electrode. The above explanation of the phenomenon appeared here can be supported by the results reported by Yu Shen et al [51].

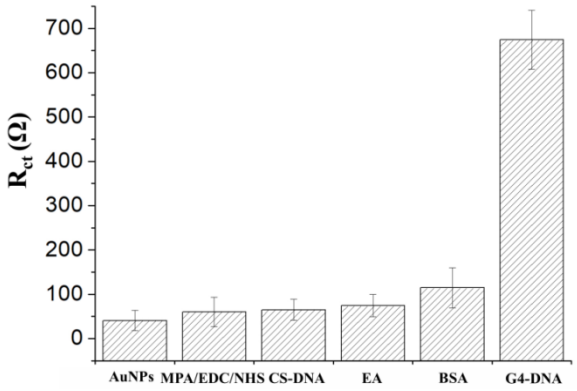

Figure 4. Changes in Rct after the electrodes were functionalized with AuNPs, MPA/EDC/NHS, CS-DNA, EA, BSA and G4-DNA.

3.3 Optimization of the aptasensor

Optimization of the aptasensor was carried out to ensure that the optimal parameters were selected for the determination of Pb(II). The change in the relative Rct was measured by altering the length of CS-DNA (the number of base pairs) and the incubation time. The length of CS-DNA in the duplex played an important role in the sensitivity of the aptasensor for determining the Pb(II) concentration. The relative Rct values of 1 μg/L Pb(II) were measured using the proposed aptasensor with CS-DNA containing different amounts of base pairs, as shown in Fig. 5A. The relative Rct increased with the increase in the number of base pairs over the range of 5 to 11 and then decreased in the range of 11 to 15. This result was because the bond between CS-DNA and G4-DNA could be enhanced by increasing the complementary base pairing between A and T and C and G, which resulted in more G4-DNA being easily immobilized on the electrode at room temperature. However, when the number of base pairs exceeded 11, the complementary base pairing between CS-DNA and G4-DNA was so strong that G4-DNA could not be easily detached from CS-DNA after being exposed to Pb(II). The results shown in this section was in good agreement with the finding presented by Hui Wang et al, which indicating an obvious relationship between the number of base pairs and relative Rct values [52]. Furthermore, there was no significant change in the relative Rct after the aptasensor was incubated in 1 μg/L Pb(II) with a CS-DNA length of 16 base pairs, demonstrating that there was no structural conversion caused by the induction of Pb(II). This result was primarily because at room temperature, the formed duplex DNA was hard to melt until the temperature reached 61 °C. It is generally known that incubation time play a key role on the binding reaction between the capture probe and target analyte [53]. Therefore, the incubation time of the aptasensor in 10 μg/L Pb(II) was optimized from 10 to 100 min, as shown in Fig. 5B. The relative Rct gradually increased from 10 to 40 min and then remained almost flat. The increase in Rct indicated that the hairpin structure of the duplex DNA composed of CS-DNA and G4-DNA was changed to a G-quadruplex by the induction of Pb(II). The steady state of the

relative Rct might be due to Pb(II), at a concentration of 10 μg/L, being saturated on the aptamer-modified electrode surface. Therefore, an incubation time of 40 min was chosen as the optimal value.

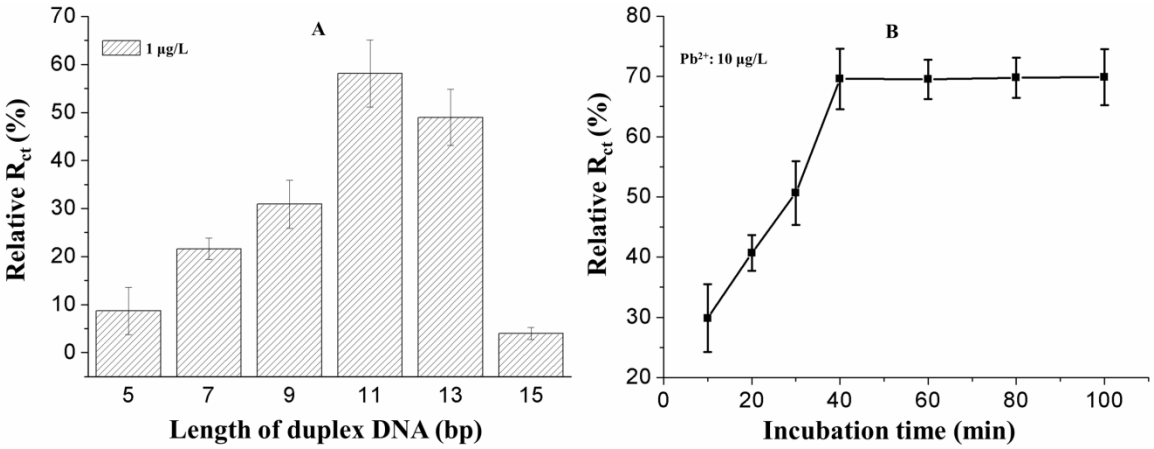

Figure 5. Effect of the CS-DNA length in the duplex on the relative Rct of 1 μg/L Pb(II) (A), and the effect of the incubation time on the relative Rct of 10 μg/L Pb(II).

3.4 Selectivity and stability of the aptasensor

As one of the important parameters used for the characterization of the biosensors, the selectivity of the proposed aptasensor was investigated under optimal conditions, as shown in Fig. 6A, by measuring the relative Rct of 10 μg/L Pb(II) in different metal ion solutions, such as Na^+, K^+, Mg^{2+}, Cu^{2+}, Cd^{2+}, Ca^{2+}, Zn^{2+} and Fe^{2+} at concentrations 100 times higher than that of Pb(II), under optimal conditions. The results indicated that the relative Rct of 10 μg/L Pb(II) measured by the proposed aptasensor was not significantly influenced by the nontargeted ions mentioned above because the mean values of the relative Rct measured in the presence of the nontargeted ions were within the relative Rct range measured with only Pb(II) (± double standard deviation (SD)). The outstanding selectivity of this aptasensor could be ascribed to the specific identification of the aptamer to Pb(II) with the formation of the G-quadruplex, which can be verified by the previous reports with similar results [54-57].

As shown in Fig. 6B, to evaluate the reproducibility and stability of the proposed aptasensor for the determination of Pb(II), five EIS measurements with 1 μg/L Pb(II) were performed using the same aptasensor. The aptasensor was activated after each determination by again immobilizing G4-DNA with a 40-min incubation. The results of the five repeated measurements are shown in Fig. 6B, which indicated that the proposed aptasensor had good reusability because the relative Rct values of the five determinations were almost unchanged and the relative SD of the five repeated measurements for Pb(II) was 1.78 %, which was under 5 %. Wenyong Hu et al. developed an aptasensor for copper detection, which also used the relative SD to validate the reliability and reproducibility of their proposed sensor [58].

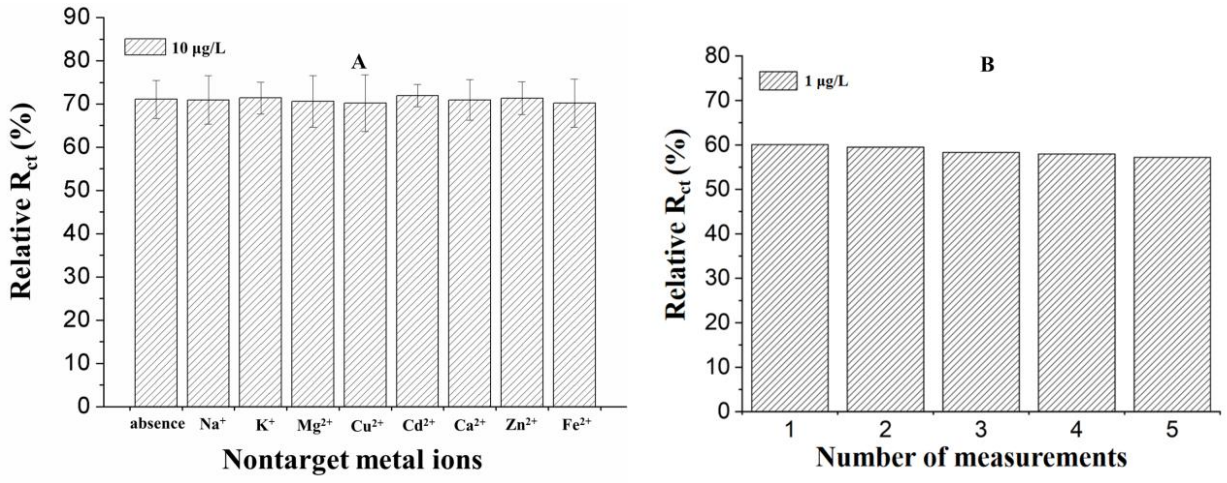

Figure 6. Selectivity study of the relative Rct with 10 μg/L Pb(II) in the presence of different metal ions at concentrations 100 times higher than that of Pb(II) (A). Five repeated measurements with 1 μg/L Pb(II) using the proposed aptasensor (B).

Moreover, the effect of the G4-DNA base sequence on the sensing performance of Pb(II) at concentrations of 100 and 0.01 μg/L was also investigated, as shown in Fig. 7. There was no significant change in the relative Rct in solutions of 0.01 μg/L Pb(II) and 100 μg/L Pb(II) when the base sequence of G4-DNA was changed, which was called NS-DNA. This result indicated that the G4-DNA designed in this specific base sequence could effectively bind with Pb(II) compared with other base sequences, e.g., NS-DNA. Marta Jarczewskaa et al. demonstrated that the base sequence of DNA has a significant influence on the capability of aptamer conformation switch, which enables its specific binding to the target analyte [53].

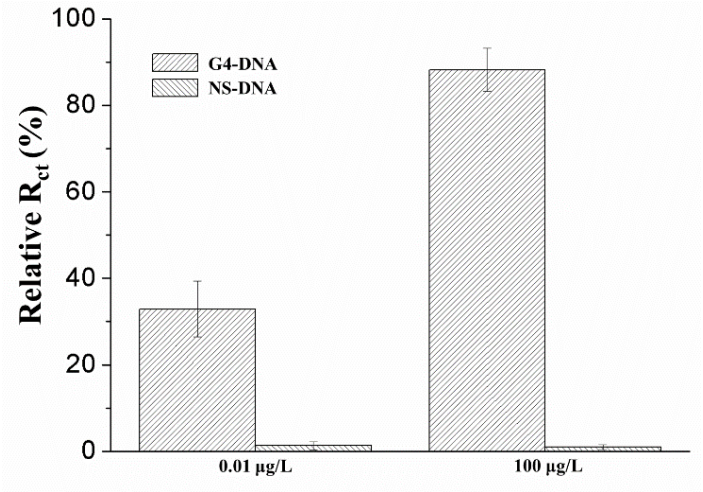

Figure 7. Effect of the base sequence on the sensing performance of the aptasensor with 0.01 and 100 μg/L Pb(II).

3.5 Analytical performances

Additionally, we investigated the relationship between the concentrations of Pb(II) and the relative Rct over a concentration range of 1 to 10^5 ng/L, as shown in Fig. 8. The relative Rct was measured by the EIS simulation under optimal conditions. The EIS responses of Pb(II) after simulating with different concentrations of Pb(II) are shown in Fig. 8A. Furthermore, the relationship between the Pb(II) concentrations and the values of the relative Rct can be distinctly observed in Fig. 8B. The value of the relative Rct decreased with an increasing Pb(II) concentration, which demonstrated that the DNA duplex structure was converted into the G4 single-strand structure by the induction of Pb(II) and finally resulted in the detachment of the G-quadruplex-Pb(II) conjugate.

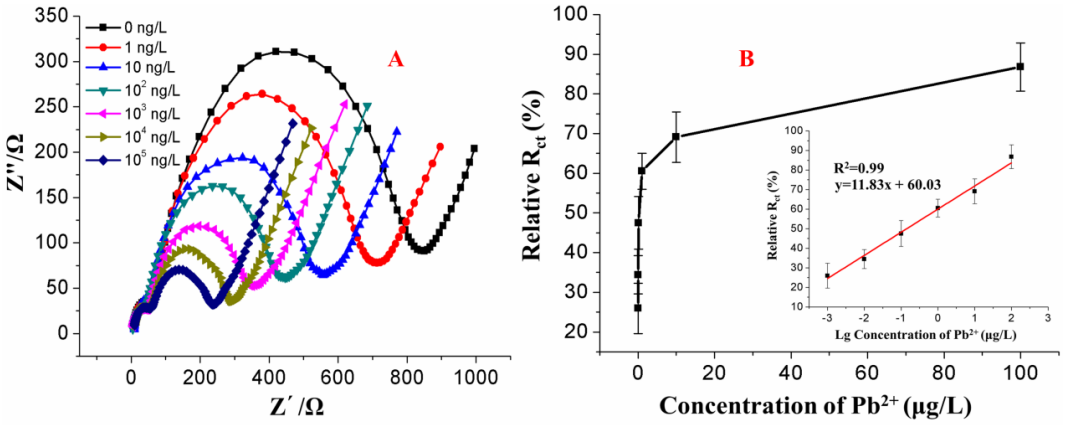

Figure 8. Nyquist curves for the different concentrations of Pb(II) (A). Calibration curve for detecting Pb(II) (B).

A linear relationship between the logarithm of the Pb(II) concentration over the range of 1 to 10^5 ng/L and the values of the relative Rct is shown in the inset of Fig. 8B. A regression equation was set up as y = 11.83 log (x) + 60.03 (x: Pb(II) concentration, y: related Rct) with a correlation coefficient of 0.99. The similar liner relationship between logarithm of target analyte concentration and the values of the relative Rct was also found in the other published papers [51,60], which reflected the feasibility of the aptasensor proposed in this study from another point of view. The limit of detection was calculated to be 0.0046 nM at a signal-to-noise ratio of 3.

The electrochemical aptasensor developed in this study could be expected to be a new alternative to the current analysis methods for the detection of Pb(II) because this aptasensor had a quick response, low limit of detection and good reusability. The distinguished features of the developed aptasensor enabled it to have a satisfactory detection performance compared with that of other aptasensors [54-57,59-66]. The comparison of the detection performance between the proposed aptasensor in this paper and previously reported sensors is shown in Table 1. The results listed in Table 1 indicate that the analytical performance of the proposed Aptamer/AuNPs/GCE aptasensor, i.e., the detection range and detection limit, was comparable and even better than previously reported sensors [59-65,54,55], which could be reused by reactivating the sensing layer after rebinding G4-DNA. Several reported aptasensors showed in Table 1 have a similar detection limit to this work [56,57,66]. However, the preparation and

use of these sensors were more tedious than that undertaken in this work. Additionally, they were not capable to be reused. Our future investigation will focus on improving the sensing layers modified on the electrode surface, as well as the miniaturization of the electrode that will be modified with a sensing layer and receptor.

Table 1. Comparison of the different aptamer-based sensors for Pb(II) determination.

Sensor	Method	Linear range	Detection limit	Reference
DNA-modified GCE	DPV	50-105 nM	4.2 nM	[59]
DNA-modified gold electrode	EIS	0.5-50000 nM	0.5 nM	[60]
T-C/DenAu/Au	DPV	0.1-100 nM	0.075 nM	[61]
Oligonucleotide/gold disk electrode	SWV	50-1000 nM	34.7 nM	[62]
Gold nanoparticles-DNAzyme	Colorimetric	3-100 nM	3 nM	[63]
DNAzyme-Aptamer	Fluorescent	0-25000 nM	4 nM	[64]
RGO/CdS/Aptamer	Photoelectrochemical	0.1-50 nM	0.05 nM	[65]
Electrochemical aptasensor	DPV	0.1-1000 ng/mL	0.03 ng/mL	[54]
AuNPs-Apt-CS-SPGE	DPV	0.6 nM-100 nM	312 pM	[55]
Paper-based aptasensor	Fluorescence	5-70 pM and 0.07-20 nM	0.5 pM	[56]
CNNFs-Ru(phen)$_3^{2+}$ aptasensor	ECL	0.1 pM-10 nM	0.04 pM	[57]
Au@p-rGO/GCE	Amperometric curves	5 pM-1 μM	1.67 pM	[66]
Aptamer/AuNPs/GCE	EIS	0.005-5000 nM	0.0046 nM	This paper

4. CONCLUSIONS

A label-free electrochemical aptasensor for the sensitive detection of Pb(II) was developed in this study. The configuration of the G4-DNA could be regulated by Pb(II) to form a hairpin G-quadruplex, which contributed to the enhanced sensing signal and improved sensitivity. A AuNP layer was electrodeposited on the surface of a GCE as a self-assembled monolayer to increase the specific surface area and number of active sites for the immobilization of CS-DNA. The CS-DNA modified on AuNPs/GCE was used as a specific receptor for the immobilization of G4-DNA. This developed aptasensor for the detection of Pb(II) offers a new general platform with improved sensitivity; moreover, the proposed aptasensor could be reused by rebinding with G4-DNA. Additionally, the proposed sensor revealed a satisfactory selectivity for Pb(II) over other metal ions attributed to the specific interaction between the aptamer and Pb(II). The aptasensor developed in this paper provides a new alternative tool for the sensitive and selective detection of Pb(II) and is expected to have potential applications in the environmental and biomedical fields.

ACKNOWLEDGEMENTS
This work was supported by the National Natural Science Foundation of China (No. 32001411), the Foundation for Distinguished Young Talents, Nanjing Agricultural University (No. 603690) and the General Program of the National Natural Science Foundation of China (No. 32071898).

DECLARATION OF INTEREST
The authors have no conflicts of interest to declare.

References

1. M. Tüzen, *Food Chem.*, 80 (2003) 119.
2. S. Birghila, S. Dobrinas, G. Stanciu, A. Soceanu, *Environ. Eng. Manag. J.*, 7 (2008) 805.
3. G. Aragay, A. Merkoçi, *Electrochim. Acta*, 84 (2012) 49.
4. M. B. Gumpu, S. Sethuraman, U. M. Krishnan, J. B. B. Rayappan, *Sens. Actuators, B*, 213 (2015) 515.
5. G. Aragay, J. Pons, A. Merkoçi, *J. Mater. Chem.*, 21 (2011) 4326.
6. N. Lewen, S. Mathew, M. Schenkenberger, T. Raglione, *J. Pharmaceut. Biomed.*, 35 (2004) 739.
7. A. A. Ammann, *Anal. Bioanal. Chem.*, 372 (2002) 448.
8. C. Moor, T. Lymberopoulou, V. J. Dietrich, *Microchim. Acta*, 136 (2001) 123.
9. A. Salvo, N. Cicero, R. Vadalà, A. F. Mottese, D. Bua, *Nat. Prod. Res.*, 30 (2016) 657.
10. W. Yantasee, Y. Lin, K. Hongsirikarn, G. E. Fryxell, R. Addleman, C. Timchalk, *Environ. Health Persp.*, 115 (2007) 1683.
11. D. Pan, Y. Wang, Z. Chen, T. Lou, W. Qin, *Anal. Chem.*, 81 (2009) 5088.
12. N. Verma, M. Singh, *Biometals*, 18 (2005) 121.
13. R. Joshi, H. Janagama, H. P. Dwivedi, T. S. Kumar, L. A. Jaykus, J. Schefers, S. Sreevatsan, *Mol. Cell. Probe.*, 23 (2009) 20.
14. T. Li, L. Shi, E. Wang, S. Dong, *Chem. Eur. J.*, 15 (2009) 1036.
15. J. K. Herr, J. E. Smith, C. D. Medley, D. Shangguan, W. Tan, *Anal. Chem.*, 78 (2006) 2918.
16. N. Hamaguchi, A. Ellington, M. Stanton, *Anal. Biochem.*, 294 (2001) 126.
17. L. Farzin, M. Shamsipur, S. Sheibani, *Talanta*, 174 (2017) 619.
18. L. Zhou, L. J. Ou, X. Chu, G. L. Shen, R. Q. Yu, *Anal. Chem.*, 79 (2007) 7492.
19. T. Mairal, V. C. Özalp, P. L. Sánchez, M. Mir, I. Katakis, C. K. O'Sullivan, *Anal. Bioanal. Chem.*, 390 (2008) 989.
20. S. Song, L. Wang, J. Li, C. Fan, J. Zhao, *TrAC Trend. in Anal. Chem.*, 27 (2008) 108.
21. L. Barthelmebs, A. Hayat, A. W. Limiadi, J. L. Marty, T. Noguer, *Sens. Actuators, B*, *156* (2011) 932.
22. S. Xie, Y. Chai, Y. Yuan, L. Bai, R. Yuan, *Biosens. Bioelectron.*, 55 (2014) 324.
23. J. A. Lee, S. Hwang, J. Kwak, S. I. Park, S. S. Lee, K. C. Lee, *Sens. Actuators, B*, 129 (2008) 372.
24. Z. Lin, L. Chen, G. Zhang, Q. Liu, B. Qiu, Z. Cai, G. Chen, *Analyst*, 137 (2012) 819.
25. H. Pei, F. Li, Y. Wan, M. Wei, H. Liu, Y. Su, C. Fan, *J. Am. Chem. Soc.*, 134 (2012) 11876.
26. A. Noori, S. Centi, S. Tombelli, M. Mascini, *Anal. Bioanal. Electrochem.*, 2 (2010) 178.
27. E. Farjami, R. Campos, J. S. Nielsen, K. V. Gothelf, J. Kjems, E. E. Ferapontova, *Anal. Chem.*, 85 (2012) 121.
28. F. J. Mearns, E. L. Wong, K. Short, D. B. Hibbert, J. J. Gooding, *Electroanal.*, 18 (2006) 1971.
29. R. Campos, A. Kotlyar, E. E. Ferapontova, *Langmuir*, 30 (2014) 11853.
30. J. Prakash, H. Joachin, *Electrochim. Acta*, 45 (2000) 2289.
31. J. Wang, R. Polsky, D. Xu, *Langmuir*, 17 (2001) 5739.
32. J. Wang, D. Xu, R. Polsky, *J. Am. Chem. Soc.*, 124 (2002) 4208.

33. O. Lioubashevski, V. I. Chegel, F. Patolsky, E. Katz, I. Willner, *J. Am. Chem. Soc.*, 126 (2004) 7133.
34. P. C. Biswas, Y. Nodasaka, M. Enyo, M. Haruta, *J. Electroanal. Chem.*, 381 (1995) 167.
35. A. Yu, Z. Liang, J. Cho, F. Caruso, *Nano Lett.*, 3 (2003) 1203.
36. R. A. Reynolds, C. A. Mirkin, R. L. Letsinger, *J. Am. Chem. Soc.*, 122 (2000) 3795.
37. R. Jin, G. Wu, Z. Li, C. A. Mirkin, G. C. Schatz, *J. Am. Chem. Soc.*, 125 (2003) 1643.
38. H. Cai, C. Xu, P. He, Y. Fang, *J. Electroanal. Chem.*, 510 (2001) 78.
39. X. Yang, J. Xu, X. Tang, H. Liu, D. Tian, *Chem. Commun.,* 46 (2010) 3107.
40. J. Liu, Y. Lu, *J. Am. Chem. Soc.*, 125 (2003) 6642.
41. J. H. Kim, S. H. Han, B. H. Chung, *Bios. Bioelectron.*, 26 (2011) 2125.
42. D. Zhang, L. Yin, Z. Meng, A. Yu, L. Guo, H. Wang, *Anal. Chim. Acta*, 812 (2014) 161.
43. H. Hai, F. Yang, J. Li, *RSC Adv.*, 3 (2013) 13144.
44. G. Liang, X.H. Liu, *Microchim. Acta*, 182 (2015) 2233.
45. G. Liang, Y. Man, X. Jin, L. Pan, X. Liu, *Anal. Chim. Acta*, 936 (2016) 222.
46. R. G. Cao, B. Zhu, J. Li, D. Xu, *Electrochem. Commun.*, 11 (2009) 1815.
47. S. Chung, J. M. Moon, J. Choi, H. Hwang, Y. B. Shim, *Biosens. Bioelectron.*, 117 (2018) 480.
48. J. Kang, X. Li, G. Wu, Z. Wang, X. Lu, *Anal. Biochem.*, 364 (2007) 165.
49. J. Wang, W. Meng, X. Zheng, S. Liu, G. Li, *Biosens. Bioelectron.*, 24 (2009) 1598.
50. Q. Xu, X. Lou, L. Wang, X. Ding, H. Yu, Y. Xiao, *ACS Appl. Mater. Interfaces*, 8 (2016) 27298.
51. Y. Shen, T. T. Tran, S. Modha, H. Tsutsui, A. Mulchandani, *Biosens. Bioelectron.*, 130 (2019) 367.
52. H. Wang, Y. Liu, G. Liu, *Microchim. Acta*, 185 (2018) 142.
53. M. Jarczewska, J. Rębiś, Ł. Górski, E. Malinowska, *Talanta*, 189 (2018) 45.
54. G. Ran, F. Wu, X. Ni, X. Li, X. Li, D. Liu, J. Sun, C. Xie, D. Yao, W. Bai, *Sens. Actuators, B*, (2020) 128326.
55. S. M. Taghdisi, N. M. Danesh, P. Lavaee, M. Ramezani, K. Abnous, *Sens. Actuators, B*, 234 (2016) 462.
56. Z. Khoshbin, M. R. Housaindokht, M. Izadyar, A. Verdian, M. R. Bozorgmehr, *Anal. Chim. Acta*, 1071 (2019) 70.
57. 57.Y. Peng, Y. Li, L. Li, J. J. Zhu, *J. Hazard. Mater.*, 359 (2018) 121.
58. W. Hu, X. Min, X. Li, S. Yang, L. Yi, L. Chai, *RSC Adv.*, 6 (2016) 6679.
59. A. Bala, M. Pietrzak, Ł. Górski, E. Malinowska, *Electrochim. Acta*, 180 (2015) 763.
60. Z. Lin, Y. Chen, X. Li, W. Fang, *Analyst*, 136 (2011) 2367.
61. F. Li, L. Yang, M. Chen, P. Li, B. Tang, *Analyst*, 138 (2013) 461.
62. M. Jarczewska, E. Kierzkowska, R. Ziółkowski, Ł. Górski, E. Malinowska, *Bioelectrochemistry*, 101 (2015) 35.
63. Z. Wang, J. H. Lee, Y. Lu, *Adv. Mater.*, 20 (2008) 3263.
64. Y. Xiang, A. Tong, Y. Lu, *J. Am. Chem. Soc.*, 131 (2009) 15352.
65. Y. Zang, J. Lei, Q. Hao, H. Ju, *ACS appl. Mater. Inter.*, 6 (2014) 15991.
66. S. M. Taghdisi, N. M. Danesh, P. Lavaee, M. Ramezani, K. Abnous, *Sens. Actuators, B*, 234 (2016) 462.